Photoelectron Spectrum of Ammonia, a Test Case for the Calculation of Franck−Condon Factors in Molecules Undergoing Large Geometrical Displacements upon Photoionization†

Andrea Peluso,* Raffaele Borrelli, and Amedeo Capobianco

Dipartimento di Chimica, Università di Salerno, I-84084 Fisciano, Salerno, Italy

Received: May 28, 2009; Revised Manuscript Received: June 19, 2009

The vibrational structure of the photoelectron spectrum of ammonia, the simplest molecule undergoing a large displacement of its equilibrium geometry upon photoionization, is analyzed by evaluating the Franck−Condon integrals at the anharmonic level of approximation. It is shown that if the rectilinear Cartesian representation of normal modes is adopted Duschinsky's transformation yields a too large displacement of the bond distance coordinate, with the appearance of several progressions which are not observed in the experimental spectrum. This apparent failure is completely corrected by the inclusion of anharmonic couplings between the principal active mode, the out of plane bending of the planar cation, and the totally symmetric stretching mode, leading to a satisfying reproduction of the observed spectrum and to a more convincing assignment of the weaker progression observed in the high-resolution spectrum.

Introduction

Ammonia is a very interesting molecule for experimental and theoretical spectroscopists. On one hand, it is a prototype of floppy molecules[1−3] because in the ground electronic state it exhibits two distinct equilibrium nuclear configurations, which interconvert each other along a large amplitude motion, the so-called umbrella motion. The inversion motion causes the splitting of all the rovibrational energy levels, thus providing a set of experimental data useful for testing the accuracy of sophisticated theoretical models for treating strong anharmonic effects.[4,5] On the other hand, ammonia is among the smallest molecules which undergo significantly large displacements of their equilibrium nuclear geometries upon excitation. Those displacements reflect into very broad absorption bands, often characterized by long, well-resolved vibrational progressions, which are of difficult assignment because they involve highly excited vibrational states, whose wave functions could be significantly affected by anharmonic effects. Indeed, ammonia presents broad absorptions both in the electronic and in the photoelectron spectra,[6−8] one of which, the well-resolved $^2A_1'' \leftarrow \tilde{X}^1A_1$ transition, observed in the gas-phase photoelectron spectrum of ammonia (Figure 1), has been a matter of controversial point of views.

In this paper, we will afford, once again, the calculation of the Franck−Condon factors for this electronic transition. The reason for resuming such an old problem is connected with the fact that in the past the best agreement with the experimental results has been obtained by using approaches which do not make use of the normal modes of both electronic states and therefore of the Duschinsky transformation between them.[9−12] Since Duschinsky's transformation is a very powerful tool for understanding radiative and nonradiative electronic transition, we believe that a better understanding of the reasons of this apparent failure in such a simple case as ammonia, as well as the attempt of finding out possible solutions, is in order.

It is well-known that in the case an electronic transition takes place between two states exhibiting a large displacement of their equilibrium positions the calculation of Franck−Condon (FC) factors may pose problems, especially when the rectilinear Cartesian representation of normal modes is adopted.[13,14] That happens because in rectilinear coordinates a large displacement along a bending coordinate always implies a motion along a stretching coordinate.[15] Indeed, in the case of the V ← N transition of ethylene, calculation of FC factors carried out in harmonic approximation and employing the Cartesian representation of normal modes led to a computed spectrum which was structureless and broad, characterized by a bandwidth much larger than its experimental counterpart.[14] The broadness was due to the appearance of vibrational progressions of the torsional mode with the simultaneous excitation of the symmetric CH stretching normal mode, to which Duschinsky's transformation of normal modes in Cartesian representation assigns a large equilibrium position displacement. This large displacement has no experimental counterpart; neither vibrational progressions have been assigned to this mode nor the resonance Raman

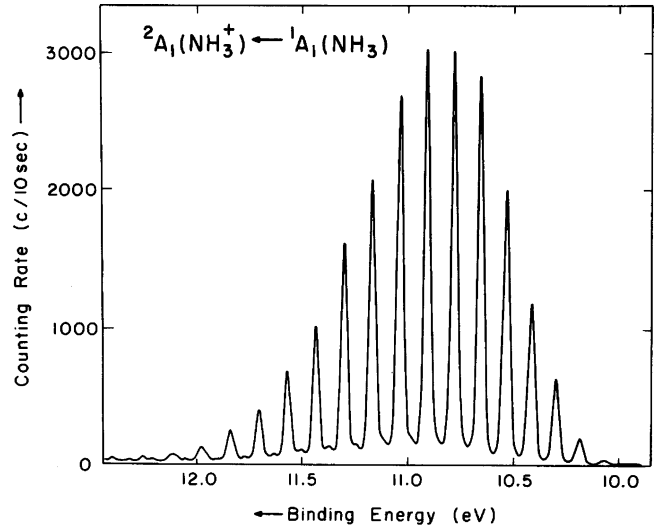

Figure 1. Lowest energy band of the photoelectron spectrum of ammonia, reproduced with permission from Rabalais et al. (*J. Chem. Phys.* **1973**, *58*, 3370−3372).

† Part of the "Vincenzo Aquilanti Festschrift".

* Corresponding author. E-mail: apeluso@unisa.it.

10.1021/jp905004z
Published on Web 07/14/2009

spectrum indicated any significant change in the CH bond length.[16] As for ammonia, even in the case of ethylene, approaches which do not make use of the normal modes of both electronic states give better results.[17,18] However, for ethylene it was sufficient to resort to the internal coordinate representation of normal modes for obtaining a theoretical spectrum whose shape nicely agreed with the experimental data,[14] but it must be noted that for ethylene the complexity of the spectrum, with the presence of a continuum structure at lower wavelengths, does not allow for a definitive assignment of all the vibronic peaks.[19]

The $^2A_1'' \leftarrow \tilde{X}^1A_1$ transition of ammonia is more intriguing and represents a much better test case for the computation of FC factors because it exhibits a high resolved spectrum, without any overlapping continuum, which could make difficult an unambiguous assignment of all the peaks. Noteworthy, for the photoelectron spectrum of ammonia, the adoption of the curvilinear representation of normal modes improved the theoretical spectrum but still left significant differences with the experimental one.[20] Here we will mainly focus on the use of the Cartesian representation of normal modes, showing that the experimental spectrum can be reproduced with a high accuracy by considering the strong anharmonic couplings between the totally symmetric stretching mode and the bending mode.

Photoelectron Spectrum of Ammonia

The ground electronic state of ammonia is $^1A_1$, with an electronic configuration

$$1a_1^2 2a_1^2 1e^4 3a_1^2$$

so that its photoelectron spectrum consists of two transitions, a lower energy one, corresponding to the removal of an electron from the least tightly bound $3a_1$ orbital, the nitrogen lone pair, and a higher-energy one corresponding to the removal of a 1e electron.[7] The higher-energy absorption, the $^2E \leftarrow \tilde{X}^1A_1$ transition, consists of a broad absorption, with two series of discrete peaks superimposed on a continuum curve, whereas the lower energy one, the $^2A_1'' \leftarrow \tilde{X}^1A_1$ transition, exhibits a long vibrational progression, extending over about 2 eV and consisting of 16 well-resolved vibrational peaks, with the maximum intensity occurring at the seventh peak (see Figure 1).[8]

The first absorption peak is very weak, thus indicating that photoionization significantly affects the equilibrium geometry of the ammonia cation. Since the outermost a_1 molecular orbital is a nonbonding orbital, the removal of an electron from it should not affect either the 3-fold symmetry of the molecule or the N−H bonding distance, and thus the vibrational progression was assigned to the ν_2 normal mode of vibration, Herzberg's notation,[21] along which umbrella motion takes place. The observed vibrational spacings, of the order of 0.12 eV (970 cm^{-1}), further support that assignment. The strict similarity between the intensity distribution of the vibrational states of the photoelectron spectrum with that of the UV absorption at 2168 Å, whose upper electronic state is known to be planar from the analyses both of the vibrational pattern[22] and of the rotational fine structure of some vibronic peaks,[23] led to the conclusion that the $^2A_1$ ionic state of ammonia has a planar equilibrium nuclear configuration, belonging to the D_{3h} point group.

The first attempts to better rationalize the spectrum through the computation of Franck−Condon factors were quite unsuccessful.[20,24,25] The main problem was with the intensity distribution and in particular with the location of the most intense peak, which theoretical calculation of FC factors predicted to be the fifth one rather than the seventh. The geometry of the neutral molecule was known with good accuracy,[26] and also the planar nuclear configuration of the molecular cation was well assessed, thus the only geometrical parameter which could be responsible for that discrepancy was the N−H bond length. The intensity distribution significantly depends on the N−H distance. Botter and Rosenstock showed that by assuming no bond length changes the computed spectrum contains significant contribution from states arising from the simultaneous excitation of the symmetric stretching mode and the symmetric bending mode, a sort of vibronic combination bands.[24] Those transitions could change the intensity distribution of the computed peaks in the higher-energy region, on the assumption that the frequency of the symmetric stretching mode (ν_1) of the planar cation is a nearly integral multiple of the bending one (ν_2).[25,20] However, the high resolution spectrum recorded by Rabalais et al. (see Figure 1) and more recently by Edvardsson et al. does not support such a hypothesis. The spectrum consists of a strong progression, due to excitation of only the bending mode, accompanied by a much weaker but well-resolved progression, falling at higher energy. The most intense peak was the eighth one,[8,27] but the origin of the band at the lowest energy was uncertain: it could be either the $0' \leftarrow 0$ transition or a hot band involving those vibrational states of the molecular cation with larger FC factors. While Rabelais et al. left this question open, the fine structure of that band obtained by Edvardsson et al. supports the hypothesis of a hot band.

A better agreement between the predicted and the observed intensity distribution was obtained by Domcke et al., who used a somewhat different approach.[10] They expanded the potential energy hypersurface of the cationic state around the equilibrium geometry of the neutral state, without computing the normal modes of the final state. The FC factors are then expressed in terms of quantities which are given by the first and higher-order derivatives of the two potential energy surfaces with respect to the normal coordinates of the initial state, evaluated at the equilibrium geometry of the latter. The spectrum computed in this way agrees much better with the experimental one, but peak intensities decay still too fast in the region of higher wavenumbers.

The photoelectron spectrum of NH_3 and ND_3 was also theoretically analyzed by Ågren et al., who used a one-dimensional approach using the decoupled, at first order, symmetry coordinate of the planar cation and anharmonic potentials for both the neutral and cationic state. Optimum geometries and potential energy surfaces were computed at an ab initio configuration interaction level of approximation. Even in that case, which does not make use of normal coordinates, the shape of the computed spectrum agrees well with the experimental one, but in the higher-energy region the peak intensities are significantly overestimated.[9]

Finally, at least to our knowledge, a much more sophisticated method was adopted by Domcke and coworkers, who used the multiconfigurational time-dependent Hartree method to study the internal conversion dynamics of NH_3^+ by wave packet propagation. The photoelectron spectrum was then obtained with a good accuracy by Fourier transformation of the autocorrelation function.[11,12a] The method gives satisfying results by using both the normal mode coordinates of the initial state[11] and curvilinear coordinates,[12] but in both cases Duschinsky's transformation of normal modes is avoided.

TABLE 1: Computed and Experimental Bond Lengths and Valence Angles (r_e, Å; θ_e, degrees) of NH_3 ($^1A_1$) and NH_3^+ ($^2A_1$)

	$^1A_1$				$^2A_1$	
	r_e		θ_e		r_e	
	DZ[a]	TZ	DZ	TZ	DZ	TZ
B3LYP	1.0157	1.0134	108.12	107.18	1.0286	1.0247
MP2	1.0113	1.0109	108.19	106.92	1.0213	1.0190
CC2	1.0122	1.0121	108.16	106.78	1.0217	1.0197
CCSD	1.0125	1.0115	107.85	106.77	1.0233	1.0210
MP4(SDQ)	1.0120	1.0114	107.88	106.76	1.0223	1.0203
MP4	1.0135	1.0141	107.74	106.49	1.0229	1.0216
CCSD(T)	1.0139	1.0138	107.68	106.53	1.0240	1.0224
exp.	1.0124[b]		106.67[b]		1.0145[c]	

[a] DZ is 6-31++G(d,p); TZ is 6-311++G(3df,3pd). [b] Ref 26. [c] Ref 34.

Computational Details

The structures of neutral and cationic ammonia obtained at different levels of approximation—density functional theory (DFT), Mœller−Plesset perturbation theory (MP), coupled cluster with single and double excitations (CCSD) and its approximation CC2, and CCSD(T), i.e., CCSD augmented with perturbative corrections for connected triple excitations—are reported in Table 1. Computations at DFT/B3LYP, MP2, and MP4(SDQ) (MP4 with single, double, and quadruple substitutions) levels of approximation have been carried out by the Gaussian package:[28] CC2, CCSD, full MP4, and CCSD(T) calculations were performed by the ACES II package.[29]

Unrestricted formalism was adopted for the NH_3^+ radical cation. Two basis sets were employed: 6-31++G(d,p) with spherical polarization functions (hereafter DZ) and 6-311++G-(3df,3pd) (hereafter TZ). Core−valence correlation effects were included in all the calculations. Energy gradients and Hessian matrices were evaluated analytically with the only exception of the MP4(SDQ) level, where numerical derivatives of analytical gradients were used to get vibrational normal modes and harmonic frequencies.

Franck−Condon factors have been computed by using both the rectilinear Cartesian representation of normal modes and the linearized internal one. The latter has already been used in the past[20] but using values of the equilibrium nuclear coordinates different from those found by the present energy optimizations, so that computations with the new geometrical parameters have been necessary. Anharmonic calculations have been performed by using the variational method, using as the basis set a product of harmonic wave functions of the involved normal modes. Only the two totally symmetric, in C_{3v} point group, stretching and bending modes have been considered in calculations since all the other modes do not contribute to the photoelectron spectrum.

Computations of Franck−Condon factors have been carried out by using the MolFC package.[30,31] Anharmonic corrections were considered only for the cationic state because a few test computations showed that those related to the existence of a double well potential for the neutral state were small. That is because the computed lowest energy states are well described by the symmetric and antisymmetric linear combination of the two lowest energy vibrational states, without showing any significant contributions of higher-energy harmonic wave functions. From the symmetric vibrational ground state, transition to vibrational states with even quantum numbers are allowed, whereas from the antisymmetric one, states with odd quantum

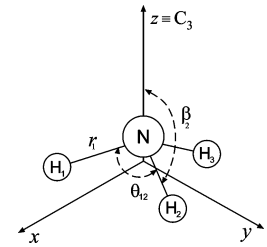

Figure 2. Internal coordinates of ammonia.

number are excited. Since the symmetric and antisymmetric vibrational modes of neutral ammonia are separated by only 0.79 cm^{-1},[3] the populations of the two levels are equal, and therefore symmetry allows the FC factors to be conveniently computed by using only one equilibrium configuration of neutral ammonia. The initial state in all the FC calculations is therefore the harmonic ground vibrational state of the neutral molecule, the only one significantly populated at room temperature.

The following symmetry adapted linear combinations of the bending coordinates have been used for both electronic states

$$\begin{cases} s_{1a} = \dfrac{1}{\sqrt{3}}(\beta_1 + \beta_2 + \beta_3) \\ s_{1e} = \dfrac{1}{\sqrt{6}}(2\theta_{12} - \theta_{13} - \theta_{23}) \\ s_{2e} = \dfrac{1}{\sqrt{2}}(\theta_{13} - \theta_{23}) \end{cases} \quad (1)$$

in conjunction with the three stretching coordinates r_i (Figure 2); β_i (eq 1) are the angles which N−H_i bonds form with the C_3 axis; and θ_{ij} are the $\angle H_iNH_j$ bending angles.[4]

Calculation of FC factors requires that the normal modes of one electronic state are expressed in terms of those of the other electronic state by means of Duschinsky's transformation

$$\mathbf{Q} = \mathbf{JQ'} + \mathbf{K} \quad (2)$$

where $\mathbf{Q},\mathbf{Q'}$ are the normal modes of the electronic states $|\psi\rangle,|\psi'\rangle$, and $\mathbf{J}$ and $\mathbf{K}$ are the rotation matrix and the equilibrium displacement vector, respectively.

If normal modes are expressed as linear combinations of the adopted nuclear coordinates, $\mathbf{S}$

$$\mathbf{Q} = \mathbf{L}^{-1}(\mathbf{S} - \mathbf{S}_0),\ \mathbf{Q'} = \mathbf{L}^{-1}(\mathbf{S} - \mathbf{S}_0) \quad (3)$$

$\mathbf{S}_0,\mathbf{S'}_0$ being the values of $\mathbf{S}$ at equilibrium geometries, expressions for $\mathbf{J}$ and $\mathbf{K}$ are easily found as follows

$$\mathbf{LQ} + \mathbf{S}_0 = \mathbf{L'Q'} + \mathbf{S}_0 \quad (4)$$

$$\mathbf{Q} = \mathbf{L}^{-1}\mathbf{L'Q'} + \mathbf{L}^{-1}(\mathbf{S}_0 - \mathbf{S'}_0) \quad (5)$$

which by comparison with eq 2 yields

$$\mathbf{J} = \mathbf{L}^{-1}\mathbf{L'},\ \mathbf{K} = \mathbf{L}^{-1}(\mathbf{S}_0 - \mathbf{S'}_0) \quad (6)$$

If normal modes of vibration are available in mass weighted Cartesian coordinates, as in the most popular packages for electronic computations, and linearized internal nuclear coor-

TABLE 2: Computed Harmonic (TZ) and Experimental Vibrational Frequencies (as Wavenumbers, cm^{-1}) of NH_3 ($^1A_1$) and NH_3^+ ($^2A_1$)

	ν_2[a]	ν_4	ν_1	ν_3
		$^1A_1$		
B3LYP	1026.96	1661.17	3470.85	3589.73
MP2	1024.93	1658.18	3532.58	3679.62
CC2	1029.25	1654.95	3515.04	3658.41
CCSD	1056.43	1676.01	3523.22	3650.46
MP4(SDQ)	1056.72	1676.34	3523.96	3653.71
MP4	1050.54	1659.61	3488.98	3623.47
CCSD(T)	1052.10	1661.78	3492.94	3621.83
exp[b]	932.43	1626.30	3336.11	3443.63
		$^2A_1$		
B3LYP	874.20	1529.29	3340.30	3514.40
MP2	865.03	1563.24	3434.61	3623.02
CC2	865.07	1560.16	3423.25	3611.57
CCSD	877.56	1560.24	3410.52	3588.71
MP4(SDQ)	873.50	1563.57	3423.12	3602.81
MP4	868.55	1555.33	3407.05	3589.01
CCSD(T)	873.19	1551.22	3392.31	3571.61
exp	903.39[c]	1507.10[d]	3232.00[e]	3388.65[f]

[a] $\nu_{1(2)}$ refers to symmetric stretching(bending). $\nu_{3(4)}$ refers to antisymmetric stretching(bending). [b] Ref 3. [c] Ref 34. [d] Ref 37. [e] Ref 38. [f] Ref 36.

dinates are adopted for FC computation, Duschinsky's transformation is a little more cumbersome[13,14]

$$\mathbf{J} = \mathbf{T}^{\dagger}\mathbf{M}^{-1/2}\mathbf{B}^{\dagger}\mathbf{G}^{-1}\mathbf{B}'\mathbf{M}^{-1/2}\mathbf{T}' \quad (7)$$

$$\mathbf{K} = \mathbf{T}^{\dagger}\mathbf{M}^{-1/2}\mathbf{B}^{\dagger}\mathbf{G}^{-1}(\mathbf{S}_0 - \mathbf{S}_0) \quad (8)$$

where $\mathbf{T}$ and $\mathbf{T}'$ are the normal mode matrices in the Cartesian representation; $\mathbf{B}$ is the transformation matrix from Cartesian to internal coordinates; and $\mathbf{G}$ is the Wilson kinetic energy matrix.[32]

Axis switching effects do not need to be considered here because of the high symmetry of the initial and final states.[1,33]

Results

The minimum energy geometries computed at different levels of approximation are reported in Table 1 and compared with the available experimental data. All the employed methods predict that the ammonia cation is planar in its ground electronic state and belongs to the D_{3h} point group. No significant changes of the NH bond distances with respect to those of the neutral state are predicted; all the methods predict a slight lengthening of the bond distance upon ionization by about 0.01 Å, slightly larger than that suggested by experimental results.[34] The MP4 and the coupled cluster methods yield the better agreement with the experimental geometry of the neutral state, and therefore we will present here only spectra computed by using geometries and normal modes obtained at the MP4(SDQ) level of computation.

In Table 2, the harmonic frequencies of the two electronic states are reported. Herzberg's notation has been adopted: ν_1 refers to the totally symmetric stretching mode of both neutral and ionized NH_3 and ν_2 to the totally symmetric bending mode of neutral ammonia, which becomes the out of plane bending mode of the cation. The ν_3 and ν_4 are the other stretching and bending normal vibrations, which are degenerate in both the neutral and the cationic ground states.

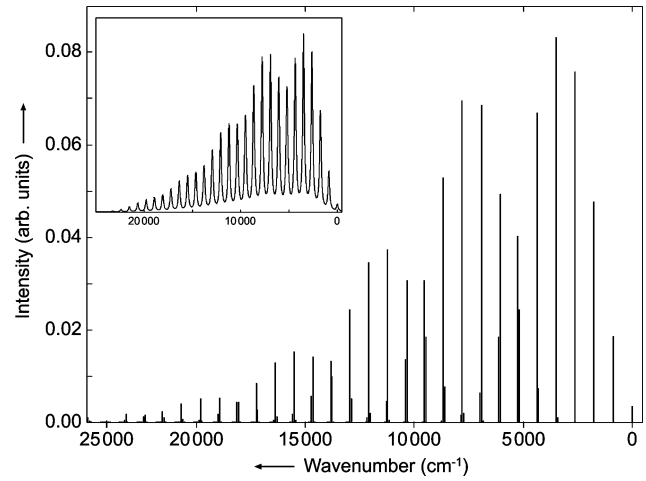

Figure 3. Franck−Condon factors computed by using the Cartesian coordinate representation and the harmonic approximation.

The hybrid B3LYP density functional method yields the best agreement between computed and experimental frequencies, but the effects due to changes of the vibrational frequencies on FC factors are largely less important than those due to geometrical changes; furthermore, the differences between DFT and MP4(SDQ) frequencies are small for the two modes which are expected to be active in the photoelectron spectrum, about 50 cm^{-1} and 30 cm^{-1} for ν_1 and ν_2, respectively.

The FC factors obtained by using harmonic approximation and the Cartesian representation of normal modes are shown in Figure 3. Five different progressions are clearly visible, each of them corresponding to progressions of the Q_2' mode with $n_1' = 0-4$. The convolution of the computed peaks with Gaussian functions is shown in the inset of Figure 3. The spectrum is much broader than the experimental one, extending over about 25 000 cm^{-1}, whereas the latter does not exceed 15 000 cm^{-1}. There are significant discrepancies between the computed and the observed spectra. Apart from the larger bandwidth, the maximum peak corresponds to the $4' \leftarrow 0$ transition for the bending mode, with $n_1' = 0$, whereas in the experimental spectrum the most intense transition is the $6' \leftarrow 0$ one.

The appearance of five progressions in the theoretical spectrum is due both to a large Duschinsky effect which mixes the symmetric bending and stretching modes, both belonging to the A_1 representation of the C_{3v} point group, and to a slight but significant component of the displacement $\mathbf{K}$ vector for the totally symmetric stretching mode. The situation is *grosso modo* similar to that already found for ethylene: Duschinsky's transformation yields a too small displacement for the bending coordinate and a too large displacement for the stretching one.[14]

The theoretical spectrum obtained by using the internal coordinate representation and harmonic approximation is reported in Figure 4. There are only two progressions: the most intense one corresponds to excitations of only the bending mode, whereas the much weaker progression corresponds to the excitation of combination bands with one quantum on the Q_1' mode. In the internal coordinate representation of normal modes, the component of the displacement vector $\mathbf{K}$ for the totally symmetric stretching mode is very small, and no Duschinsky's mixing between the bending and the stretching mode is predicted. The computed spectrum is in many aspects similar to that obtained by Harshbarger without exciting the totally symmetric stretching mode of the cationic state.[20] Although it resembles the experimental one much better than that computed by adopting the Cartesian coordinate representation, the intensity

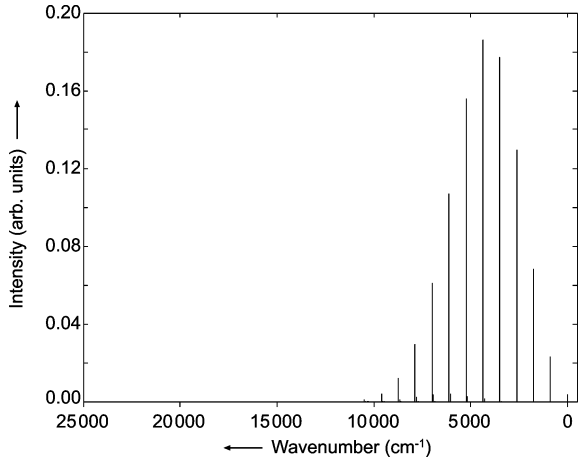

Figure 4. Franck−Condon factors computed by using the linearized internal coordinate representation and the harmonic approximation.

distribution is not well reproduced. Apart from the fact that the maximum peak height occurs for the $5' \leftarrow 0$ transition rather than for the $6' \leftarrow 0$ one, the most important discrepancies are observed in the high wavenumber region, where the computed spectrum decays much faster than the experimental one. The intensity of the higher-energy transitions is significantly underestimated, and therefore the spectrum exhibits only 12 peaks rather than the observed 16. Harshbarger, who also used the internal coordinate representation of the normal modes, included anharmonic effects too, for both the neutral and the cationic species, without significantly improving the accuracy of the theoretical results, probably because of the approximate treatment of the kinetic energy terms. Thus, in the light of previous theoretical results, there are two ways to be followed: one consisting of adopting true curvilinear coordinates with the exact treatment of the kinetic energy terms, the other being based on the Cartesian representation but with a full treatment of the anharmonic effects for the high energy states of the cationic species. Here we will focus on the latter way.

The potential energy surface as a function of the Q_1' and the Q_2' normal modes has been calculated at the MP4(SDQ)/TZ level of approximation, over a grid of about 4300 points, covering the range $0.57 \leq r \leq 1.65$ Å and $40.4° \leq \theta \leq 120°$. The potential energy has been fitted by a 16 degree polynomial, with maximum order 8 in each variable Q_1' and Q_2'. The polynomial coefficients are reported in the Supporting Information. Since in the D_{3h} point group the totally symmetric stretching and the out of plane bending belong to different irreducible representations, all the terms in odd powers of Q_2' are zero. The vibrational states have been then computed by the variational method, using analytical integrals.[35] Convergence on the lower excited vibrational states of interest has been obtained by using 40 harmonic oscillator basis functions for each mode, centered in the minimum energy position of the cationic state. Eigenstates have been computed by direct diagonalization of the Hamiltonian matrix.

The energy of low lying vibrational states is reported in Table 3 together with the available experimental data.[34,36−38] The agreement is not as good as that obtained by previous computations,[39] but it is certainly sufficient for discussing the photoelectron spectrum of ammonia. The choice of using polynomial functions for expressing the potential energy surface strongly affects the accuracy of the computed vibrational energy; however, polynomial functions greatly simplify the calculation of the FC factors, and since our main intent is that of finding

TABLE 3: Wavenumbers (cm^{-1}) and Assignments of the Lowest Excited Vibrational States of NH_3^+ at the Anharmonic Level of Approximation

ω					ω				
calc.	obs.[a]	n_1'	n_2'	coeff	calc.	obs.[a]	n_1'	n_2'	coeff
0	0	0	0	0.99	7607	−	2	1	0.95
921	903	0	1	0.99			1	3	−0.24
1873	1844	0	2	0.98	8052	7958	0	8	0.69
2852	2813	0	3	0.96			0	6	0.11
		0	5	−0.16			0	10	−0.41
3373	3232	1	0	0.98			0	12	0.10
3855	3807	0	4	0.92			1	6	−0.48
		0	6	0.20	8217	−	1	5	0.68
4286	4128	1	1	0.97			0	3	0.11
4878	4821	0	5	0.88			0	5	0.28
		0	7	−0.27			0	7	0.31
5231	−	1	2	0.94			1	7	−0.32
5920	5852	0	6	0.88			2	3	−0.41
		0	8	−0.32			2	5	−0.11
6204	6022	1	3	0.88			3	5	0.11
		0	3	0.18	8547	−	2	2	−0.91
		0	5	0.27			2	4	0.11
6704	−	2	0	0.94			1	4	−0.32
6979	6899	0	7	0.76	9139	9030	0	9	0.62
		0	9	−0.37			0	7	0.12
7200	−	1	4	0.76			0	11	−0.44
		1	6	−0.27			0	13	0.13
							1	7	−0.51

[a] From ref 39 and references therein.

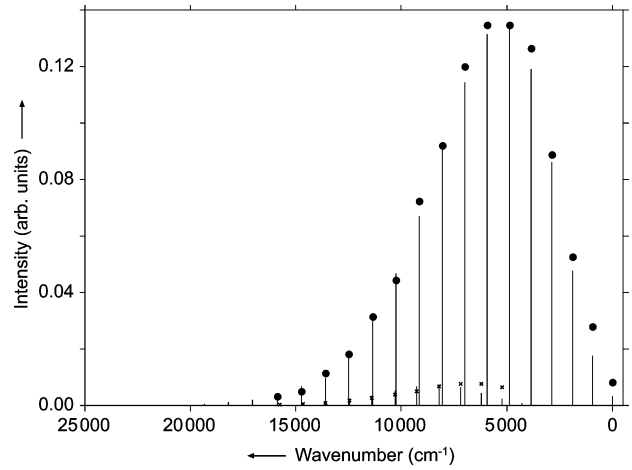

Figure 5. Franck−Condon factors computed by using the Cartesian coordinate representation and the anharmonic potential energy (l) compared with observed intensities from ref 8 (●) and from ref 27 (×).

out the most practical way for computing FC factors, to be applied to larger size molecules too, we have preferred to follow this way rather than using other approaches which have been proved to give a better accuracy on the computed frequencies.[39]

The computed FC factors are reported in Figure 5 and compared with the observed relative intensities of the high resolution spectrum of Rabelais et al.[8] The agreement between the computed and the observed spectra is satisfyingly good, concerning both the intensity distribution and the bandwidth. The whole spectrum is well reproduced, especially concerning its decay in the longer wavenumber region, which had posed problems in previous theoretical investigations.[9] The experimental bandwidth is also well reproduced by FC calculations: Rabelais' experimental spectrum shows 16 well-resolved peaks,

with a little not resolved tail, whereas the theoretical one exhibits two more, which have been indeed observed in the Edvardsson spectrum.

Because of its excellent resolution, the comparison with Edvardsson's spectrum is paradoxically more difficult because some of the peaks, but not all, show fine structures. We find a still better agreement with Edvardsson's relative intensities than with Rabelais' ones for the lower and the higher-frequency region of the spectrum, namely for those transitions which show fine structure, whereas the middle frequency region is significantly underestimated. However, the situation can be reversed if we differently scale relative intensities. By making coincident the computed and the experimental intensities of the $8' \leftarrow 0$ transition, we have a very good agreement with Edvardsson's spectrum in the middle frequency region, with a significant overestimation of all the transition occurring from the $3' \leftarrow 0$ to the $6' \leftarrow 0$.

The computed spectrum also shows the presence of a second much weaker progression, which the present FC calculation assigns to transitions to vibrational states with excitations on the bending mode Q_2' and a single quantum on the totally symmetric stretching mode Q_1', in agreement with the theoretical results of Viel et al.[11,12] That weaker progression is very well resolved in the spectrum of Edvardsson et al.,[27] and it was tentatively assigned to transitions to a vibrational progression of the asymmetric bending mode with one more quantum on the symmetric bending mode Q_2'. The first mode is of E symmetry, and therefore vibronic couplings should be invoked to justify the presence of such combination bands in the experimental spectrum.

The weak progression observed by Edvardsson et al. starts just after the sixth peak of the stronger progression, about 5400 cm^{-1} after the $0' \leftarrow 0$ transition, and exhibits a maximum for the third peak. In the computed spectrum, the weak progression also starts after the sixth peak. In Figure 5, theoretical and observed intensities are shown. The adopted scaling was the same as for the main progression; namely, we made coincident the computed and the experimental intensities of the $6' \leftarrow 0$ transition. The observed relative intensity of the highest peak of the weaker progression is 5.6%, and the computed value is 5.3%. The good agreement therefore supports our assignment.

The results reported in Table 3 explain why the other progressions which characterize the spectrum in harmonic approximation (see Figure 3) lose their intensity when anharmonic corrections are taken into account. Let us explicitly consider the second progression, which exhibits a maximum at about 8000 cm^{-1} for the $1',5' \leftarrow 0,0$ transition, with a high intensity, comparable with the $0',6' \leftarrow 0,0$ one. The state $|1'5'\rangle$, which has an FC integral of -0.26 with the ground vibrational state of neutral ammonia, is anharmonically coupled to a few vibrational states with $n_1' = 0$, i.e., $|0'3'\rangle$, $|0'5'\rangle$, $|0'7'\rangle$, and a few states with $n_1' = 2$, i.e., $|2'3'\rangle$, $|2'5'\rangle$, which have both positive FC integrals. Because of that, the eigenstate with the highest contribution of the $|1'5'\rangle$ harmonic state has now an FC integral with the $|00\rangle$ of only -0.085, and the corresponding FC factor decreases 1 order of magnitude upon anharmonic correction. The same reasoning applies also to the other progressions which disappear in the spectrum obtained at anharmonic level of approximation.

The intensities of the transitions occurring at lower wavenumbers are slightly underestimated, although the quality of the computed states should be higher than those at higher energy. On the assumption that the first observed band is really a hot band, as experimental and theoretical evidence leads us to suppose,[11,27] a possible explanation of the low intensity is that other peaks of such a hot progression could be hidden under the lower energy peaks. Indeed, the calculation of FC factors from the $|01\rangle$ state of neutral ammonia indicates that the transition $0'0' \leftarrow 01$ is not the most intense one, but it should be accompanied by at least four other transitions, which have still higher intensities. Those hot transitions could also affect the intensities of the peaks of the main progression making the comparison of the computed and the observed spectrum even more difficult.

Conclusion

Prediction of the band shapes for radiative transitions between electronic states with significantly different minimum energy nuclear configurations along an angular coordinate requires a little caution. In this paper we have shown that the adoption of the rectilinear Cartesian coordinate representation of normal modes requires the inclusion of higher-order anharmonic terms of the potential energy hypersurface. These terms are necessary to correct the large components of the displacement vector which Duschinsky's transformation assigns to stretching coordinates in the rectilinear coordinate representation. If the internal coordinate representation is adopted, anharmonic effects seem to play a minor role, but the dependence of the kinetic energy matrix from coordinates must be taken into account. Work is in progress along this line.

Supporting Information Available: Coefficients of the polynomial fit of the MP4(SDQ)/6-311++G(3df,3pd) potential energy of NH_3^+. This material is available free of charge via the Internet at http://pubs.acs.org.

References and Notes

(1) Houghen, J. T.; Watson, J. K. G. *Can. J. Phys.* **1965**, *43*, 298–320.
(2) Watson, J. K. G. *Mol. Phys.* **1968**, *15*, 479–490.
(3) Špirko, V.; Kraemer, W. P. *J. Mol. Spectrosc.* **1989**, *133*, 331–344.
(4) Leonard, C.; Handy, N. C.; Carter, S.; Bowman, J. M. *Spectrochim. Acta A* **2002**, *58*, 825–838.
(5) Handy, N. C.; Carter, S.; Colwell, S. M. *Mol. Phys.* **1999**, *96*, 477–491.
(6) Branton, G. R.; Frost, D. C.; Herring, F. G.; McDowell, C. A.; Stenhouse, L. A. *Chem. Phys. Lett.* **1969**, *3*, 581–584.
(7) Weiss, M. J.; Lawrence, G. M. *J. Chem. Phys.* **1970**, *53*, 214–218.
(8) Rabalais, J. W.; Karlsson, L.; Werme, L. O.; Bergmark, T.; Siegbahn, K. *J. Chem. Phys.* **1973**, *58*, 3370–3372.
(9) Ågren, H.; Reineck, I.; Veenhuizen, H.; Maripuu, R.; Arneberg, R.; Karlsson, L. *Mol. Phys.* **1982**, *45*, 477–492.
(10) Domcke, W.; Cederbaum, L. S.; Köppel, H.; Von Niessen, W. *Mol. Phys.* **1977**, *34*, 1759–1770.
(11) Viel, A.; Eisfeld, W.; Neumann, S.; Domcke, W.; Manthe, U. *J. Chem. Phys.* **2006**, *124*, 214306–214321.
(12) (a) Viel, A.; Eisfeld, W.; Evenhuis, C. R.; Manthe, U. *Chem. Phys.* **2008**, *347*, 331–339. (b) Woywod, C.; Scharfe, S.; Krawczyk, R.; Domcke, W.; Köppel, H. *J. Chem. Phys.* **2003**, *118*, 5880–5893.
(13) Reimers, J. R. *J. Chem. Phys.* **2001**, *115*, 9103–9109.
(14) Borrelli, R.; Peluso, A. *J. Chem. Phys.* **2006**, *125*, 194308–194315.
(15) Sibert, E. L.; Hynes, J. T.; Reinhardt, W. P. *J. Phys. Chem.* **1983**, *87*, 2032–2037.
(16) Sension, R. J.; Hudson, B. S. *J. Chem. Phys.* **1989**, *90*, 1337–1389.
(17) Hazra, A.; Chang, H. H.; Nooijen, M. *J. Chem. Phys.* **2004**, *121*, 2125–2136.
(18) Hazra, A.; Nooijen, M. *Phys. Chem. Chem. Phys.* **2005**, *7*, 1759–1771.
(19) Mulliken, R. S. *J. Chem. Phys.* **1955**, *23*, 1895–1907.
(20) Harshbarger, W. R. *J. Chem. Phys.* **1972**, *56*, 177–182.
(21) Herzberg, G. *Infrared and Raman Spectra of Polyatomic Molecules*; Van Nostrand Co., Inc.: Princeton, N. J., 1945.
(22) Walsh, A. D.; Warsop, P. A. *Trans. Faraday Soc.* **1961**, *57*, 345–358.
(23) Douglas, A. E. *Discuss. Faraday Soc.* **1963**, *35*, 158–174.
(24) Botter, R.; Rosenstock, H. M. *Adv. Mass. Spectrom.* **1968**, *4*, 579–588.

(25) Harshbarger, W. R. *J. Chem. Phys.* **1970**, *53*, 903–911.

(26) Morimo, Y.; Kuchitsu, K.; Yamamoto, S. *Spectrochim. Acta A* **1968**, *24*, 335–352.

(27) Edvardsson, D.; Baltzer, P.; Karlsson, L.; Wannberg, B.; Holland, D. M. P.; Shaw, D. A.; Rennie, E. E. *J. Phys. B* **1999**, *32*, 2583–2609.

(28) Frisch, M. J.; Trucks, G. W.; Schlegel, H. B.; Scuseria, G. E.; Robb, M. A.; Cheeseman, J. R.; Montgomery, J. A., Jr.; Vreven, T.; Kudin, K. N.; Burant, J. C.; Millam, J. M.; Iyengar, S. S.; Tomasi, J.; Barone, V.; Mennucci, B.; Cossi, M.; Scalmani, G.; Rega, N.; Petersson, G. A.; Nakatsuji, H.; Hada, M.; Ehara, M.; Toyota, K.; Fukuda, R.; Hasegawa, J.; Ishida, M.; Nakajima, T.; Honda, Y.; Kitao, O.; Nakai, H.; Klene, M.; Li, X.; Knox, J. E.; Hratchian, H. P.; Cross, J. B.; Adamo, C.; Jaramillo, J.; Gomperts, R.; Stratmann, R. E.; Yazyev, O.; Austin, A. J.; Cammi, R.; Pomelli, C.; Ochterski, J. W.; Ayala, P. Y.; Morokuma, K.; Voth, G. A.; Salvador, P.; Dannenberg, J. J.; Zakrzewski, V. G.; Dapprich, S.; Daniels, A. D.; Strain, M. C.; Farkas, O.; Malick, D. K.; Rabuck, A. D.; Raghavachari, K.; Foresman, J. B.; Ortiz, J. V.; Cui, Q.; Baboul, A. G.; Clifford, S.; Cioslowski, J.; Stefanov, B. B.; Liu, G.; Liashenko, A.; Piskorz, P.; Komaromi, I.; Martin, R. L.; Fox, D. J.; Keith, T.; Al-Laham, M. A.; Peng, C. Y.; Nanayakkara, A.; Challacombe, M.; Gill, P. M. W.; Johnson, B.; Chen, W.; Wong, M. W.; Gonzalez, C.; Pople, J. A. *Gaussian 03*, revision B.05, Gaussian, Inc.: Pittsburgh, PA, 2003.

(29) Stanton, J. F.; Gauss, J.; Watts, J. D.; Szalay, P. G.; Bartlett, R. J.; Auer, A. A.; Bernholdt, D. E.; Christiansen, O.; Harding, M. E.; Heckert, M.; Heun, O.; Huber, C.; Jonsson, D.; Jusélius, F.; Lauderdale, W. J.; Metzroth, T.; Michauk, C.; O'Neill, D. P.; Price, D. R.; Ruud, K.; Schiffmann, F.; Varner, M. E.; Vázquez, J. *Aces II Mainz-Austin-Budapest version*. Current version, see http://www.aces2.de.

(30) Borrelli, R.; Peluso, A. *J. Chem. Phys.* **2003**, *119*, 8437–8448.

(31) Borrelli, R.; Peluso, A. *MolFC: A program for Franck-Condon integrals calculation*. Package available online at http://www.theochem.unisa.it.

(32) Wilson, E. B.; Decius, J. C.; Cross, P. C. *Molecular Vibrations*; McGraw-Hill: New York, 1955.

(33) Özkan, I. *J. Mol. Spectrosc.* **1990**, *139*, 147–162.

(34) Lee, S. S.; Oka, T. *J. Chem. Phys.* **1991**, *94*, 1698–1704.

(35) Califano, S. *Vibrational States*; Wiley: New York, 1976.

(36) Bawendi, M. G.; Rehfuss, B. D.; Dinelli, B. M.; Okumura, M.; Oka, T. *J. Chem. Phys.* **1989**, *90*, 5910–5917.

(37) Reiser, G.; Habenicht, W.; Müller-Dethlefs, K. *J. Chem. Phys.* **1993**, *98*, 8462–8468.

(38) Bahng, M.-K.; Xing, X.; Baek, S. J.; Ng, C. Y. *J. Chem. Phys.* **2005**, *123*, 084311–084318.

(39) Yurchenko, S. N.; Thiel, W.; Carvajal, M.; Jensen, P. *Chem. Phys.* **2008**, *346*, 146–159.

JP905004Z